Springer

Journal of
Mechanical
Science and
Technology

Journal of Mechanical Science and Technology 22 (2008) 247~254

www.springerlink.com/content/1738-494x

Mode-selective ultrasonic wave sensor and its characteristics

Ho Cheol Lee*

School of Mechanical and Automotive Engineering, Catholic University of Daegu, Geumnak 1-ri, Hayang-eup, Gyeongsan-si, Gyeongsangbook-do, 712-702, Korea

(Manuscript Received October 23, 2007; Revised November 9, 2007; Accepted November 12, 2007)

Abstract

A magnetostrictive sensor is proposed that can selectively measure the specified mode among two kinds of elastic waves transmitted through a ferromagnetic shaft, and its various characteristics are examined by experiments. The magnetic circuit of the proposed sensor is configured by using permanent magnets and its mode selection is accomplished by only reversing the poles of the permanent magnets. By means of finite element analysis, the validity of the proposed sensor is verified. Prototype sensors are made and their sensitivity and linearity are investigated as basic characteristics. The results show the proposed sensors are able to measure the target mode waves with good sensitivity and linearity. By exciting undesirable modes of waves intentionally, it is verified that the sensor can measure the target modes and reject the undesirable wave modes considerably.

Keywords: Elastic wave; Magnetostrictive sensor; Mode selection

1. Introduction

Since the mid 1880's when Joule and Villari discovered magnetostriction and inverse magnetostriction, respectively, there have been numerous engineering applications utilizing these interesting phenomena [1-5]. The invention of piezoelectric materials did not reduce their value much because their energy transduction mechanisms are completely contactless.

Among their various applications, the excitation and sensing of ultrasonic waves are the most notable from the viewpoint of a noncontact characteristic [1, 6, 7]. Especially the ultrasonic waves transmitted along a shaft contain a great deal of useful information on the defects or surroundings of the shaft. The subject has drawn considerable attention and been studied by many researchers until lately [8-12].

The ultrasonic wave in a shaft can be classified into three different modes: longitudinal, flexural, and torsional. These waves have their own unique characteristics [13]. These facts tell us that it is quite useful to measure a specific mode exclusively when more than two kinds of modes are mixed.

Kwun and Teller [14] showed that various kinds of bias magnetic fields produce and measure different modes of ultrasonic waves, and Lee and Kim [15] studied sensors with mode-selective sensing capability. However, since different kinds of bias field configurations are necessary for mode selection, their works were unable to overcome the limitation of practicality.

The present paper shows that it is possible to switch one sensing mode to another by reversing the pole directions of permanent magnets under only one bias magnetic field configuration. This means that only a simple electrical switching is necessary for mode selective sensing if we change the permanent magnets with electromagnets.

The present paper can be summarized as follows. First, the principle of wave mode selection will be briefly reviewed and a new idea is proposed which makes mode-selection possible in one bias magnetic

*Corresponding author. Tel.: +82 53 850 2712, Fax.: +82 53 850 2710
E-mail address: hclee21@cu.ac.kr
DOI 10.1007/s12206-007-1107-5

configuration. Before the sensor is made, finite element analyses are done in order to verify the validity of the proposed idea. During the process, one important design guideline is presented about the distance between the permanent magnets. By making a prototype sensor, experimental verifications are carried out. The sensitivity and linearity are investigated as well. Lastly, the mode selectivity of the proposed sensor is verified by experiments.

2. Principle and analysis

2.1 Principle of wave mode selection

As is described in the former section, the recent study shows that it is possible to measure only one wave mode selectively between longitudinal and flexural waves transmitted through a ferromagnetic shaft [15]. Fig. 1 may be useful for explaining the principle. As shown, the stress distribution by mixed longitudinal and flexural waves advances to the left along a ferromagnetic shaft. We formed a bias magnetic field which is antisymmetric about the xz plane. When the stress wave passes through the bias magnetic field, a small perturbation in the magnetic field occurs by the Villari principle. The variation can be measured in the form of electrical voltages if we use a simple solenoid-type coil sensor by means of the Faraday principle. The different wave modes can be selectively measured with different bias magnetic fields. For example, under the bias magnetic field distribution of Fig. 1, the so-called antisymmetric bias magnetic field, only the flexural waves are measured. It is matter-of-course that symmetric bias magnetic fields can measure only longitudinal stress waves. It can be summarized as the similarity between bias magnetic fields and stress distributions of waves determines the mode-selection. Lee and Kim [15] show that the selective sensing is possible but cannot embody the sensor under a single sensor configuration. If it is possible to change over from one sensing mode to another by a simple operation such as an electronic switching, the sensor will be very useful in various engineering applications, for example, nondestructive online faults monitoring.

The present work proposes the device shown in Fig. 2 as a sensor with simple mode changing capability. It is found in Fig. 2 that the sensor is composed of permanent magnets for bias magnetic fields, yokes for magnetic flux paths, a solenoid-type coil sensor for converting magnetic flux variations into voltage variations. The only difference between (a) and (b) of Fig. 2 is the polarity directions of the permanent magnets. (a) is the case that its bias magnetic field has symmetry with respect to the xz plane. On the other hand, (b) is the case of antisymmetry. The former will be referred to as longitudinal sensing mode and the latter as flexural sensing mode from now on. As a result, the sensor configuration (a) measures only longitudinal waves and (b) does flexural ones. Compared with the previous sensor by Lee and Kim [15], it is not only the basic difference but also its merit that the simple exchange of the permanent magnets with electromagnets will give this sensor an electrically controlled selectivity.

It is worth noting that one problem should be checked about the bias magnetic field design of the flexural mode, which is not the case with the longitudinal mode. Fig. 3 shows the problem. As is shown in

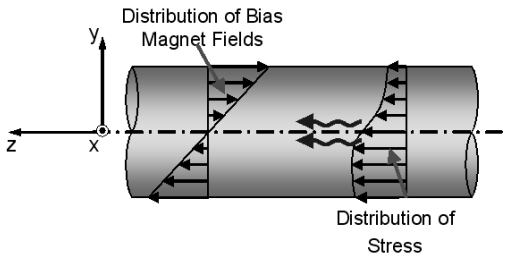

Fig. 1. Schematic for explaining the concept of wave mode selection.

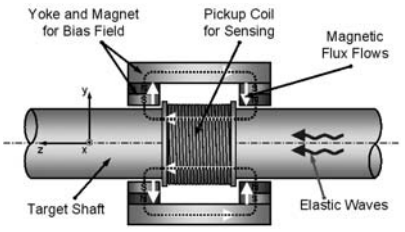

(a)

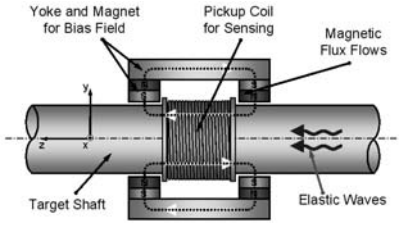

(b)

Fig. 2. Sensor configurations for measuring (a) longitudinal waves and (b) flexural waves.

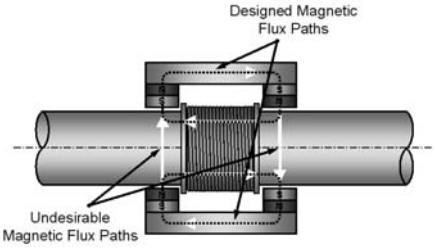

Fig. 3. Possible problem of magnetic flux leakages.

Fig. 2(a), there is no magnetic flux path across the cross section of the shaft for the longitudinal sensing mode, since the same polarities face each other. But this is not the case with the flexural sensing mode. It is illustrated in Fig. 3 that there are two main magnetic paths for the flexural sensing mode. One is the same path as the longitudinal sensing mode and the other paths pass across the cross section of the shaft. The latter is not desirable in that it does not work for sensor operations. Moreover, since the magnetic flux is divided into two paths the sensitivity of the sensor gets worse. For the sake of examining this flux leakage phenomenon systematically, it will be helpful to get its analytic model which includes the geometrical information on the magnets, the yokes, and the shaft. But its complexity makes it not practical. Instead, we utilize the finite element model to analyze this magnetic flux leakage.

2.2 Finite element analysis

The finite element model is established and analyzed with a view to examining the undesirable magnetic flux leakage problem in the flexural sensing mode. As a finite element software, ANSYS EMAG is used. The material properties and the information on the finite element model are given in Table. 1. Fig. 4(a) is the finite element model for the flexural sensing mode where the air parts are all omitted intentionally and (b) is one of its analysis results. As shown in Fig. 4(b), the majority of the magnetic flux emerging from the permanent magnets flows across the cross section of the shaft. The result suggests there will be a flux leakage problem as expected. The most important thing to be checked among the results is whether the pattern of the B_z is symmetric or antisymmetric with respect to the xz plane or not. If the pattern of the B_z is symmetric, the configuration can be used for the longitudinal wave sensing and if antisymmetric, the configuration can also be used for the flexural

Table 1. Information on the elements and material properties used by the current model.

Item	Value
Element Type	Solid97
Number of Elements	65396
Relative Permeability of Permanent Magnets	1.04
Coercive Force of Permanent Magnet	9×10^5 (A/m)
Relative Permeability of a Yoke and Shaft	500

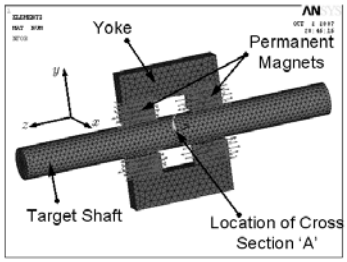

(a)

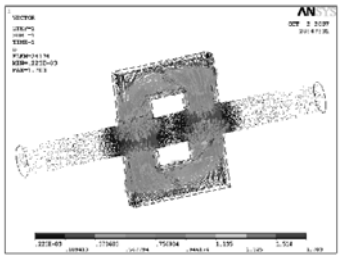

(b)

Fig. 4. (a) Finite element model of the proposed sensor and (b) results of magnetic flux density.

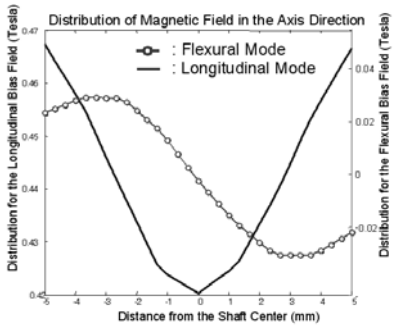

Fig. 5. Distribution of magnetic flux density B_z along the cross section for two different sensing modes.

wave sensing because the sensor can respond only when there is similarity between the bias magnetic fields and the stress distributions. In order to confirm the correct pattern, the data are extracted for how the magnetic flux density B_z in the axial direction var-

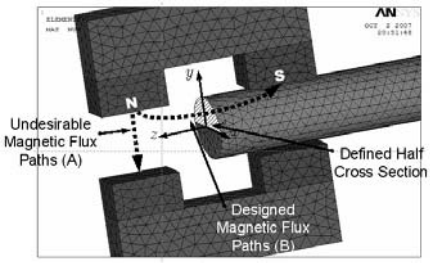

Fig. 6. Illustrative area definition and flux paths for investigating the magnetic flux leakages.

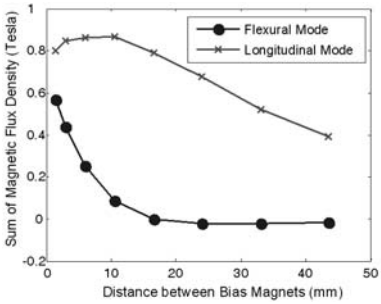

Fig. 7. Variations of the magnetic flux according to the distance between the bias magnets.

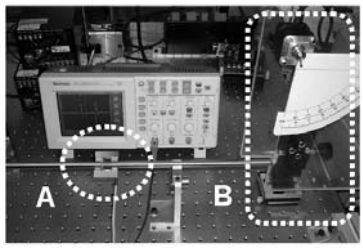

(a)

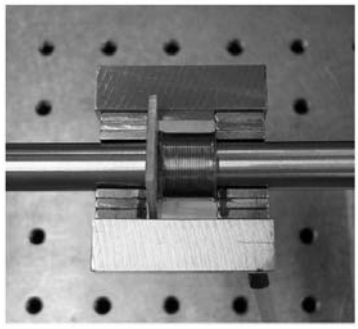

(b)

Fig. 8. (a) Experimental setup and (b) the appearance of the sensor prototype.

ies according to the y locations at the cross section illustrated as A of Fig. 4(a). The results are shown in Fig. 5. The graph shows that exactly symmetric and antisymmetric bias magnetic fields are formed across the cross section as expected.

Secondly, the problem of undesirable magnetic flux leakages is investigated. In order to quantify the extent of how much magnetic flux is leaked out, we define the half cross section at the center of two sets of the bias magnets as shown in Fig. 6. It can be said that the flux leakages are described by the total amount of magnetic flux Φ_z in the axial direction passing through this half cross section as the distance between the bias magnets varies. It is expected that the magnetic flux B_z passing through the half cross section will decrease according to the distance in all cases of longitudinal and flexural sensing mode. However, we can also expect that the reduction may be more conspicuous for the flexural case since the additional magnetic path expressed as A in Fig. 6 will lead to considerable amount of magnetic fluxes.

Using the finite element model, the total magnetic fluxes passing through the half section defined in Fig. 6 are calculated and shown in Fig. 7. The results meet our expectations in that the amounts of the magnetic flux are decreased as the bias magnets get away from each other, but the decrease is more rapid in the case of the flexural sensing mode than the longitudinal one. We can conclude that if we want to measure two kinds of wave modes in this configuration it requires that the distance between the bias magnets should be confined within a relatively short range. Otherwise, it is impossible to measure the flexural waves, or its sensitivity will not meet our requirements.

3. Experiments and characteristics

3.1 Prototyping and experiments

In order to show that the present idea of the wave mode selection is valid, prototypes are made and tested by various experiments. Fig. 8 (a) shows the experimental setup used in the test and (b) is one sample of the sensor prototypes. The simple sensor structure of Fig. 8(b) means this sensor will be cost-effective. The circle A of Fig. 8(a) indicates the location of the sensor mounting and B is the ball-drop device prepared for generating flexural or longitudinal waves independently or simultaneously. In this excitation device, the ball drops from the specified height and impacts against one end of a target shaft. This impact will make ultrasonic waves in the shaft. The permanent magnets adopted for the bias magnetic

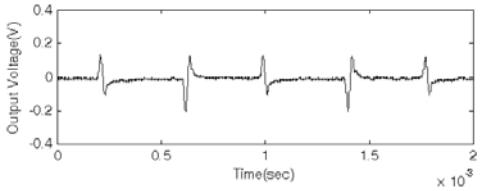

(a) Longitudinal wave mode

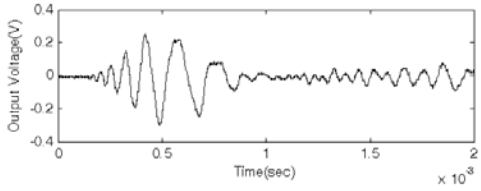

(b) Flexural wave mode

Fig. 9. Measured signals by (a) longitudinal sensing mode and (b) by flexural one.

field are Nd-Fe-B series, and the yoke for magnetic flux paths are made of S45C general steel. The number of turns of the coil sensor for measuring the magnetic flux variations is 200.

Fig. 9 (a) and (b) show the measured signals from the experiments under the longitudinal sensing mode and flexural one respectively. The non-dispersive property of longitudinal waves is well identified in Fig. 9(a). The 180 degree phase reversion ascribed to free boundary conditions of the shaft ends is also found. Fig. 9(b) is the results for the flexural sensing mode, which shows well the dispersive characteristics of flexural waves. From these results, it can be concluded that the sensor works well as expected from the finite element model.

3.2 Sensitivity

The proposed sensor has to meet some basic requirements as a meaningful sensor in order to be used in various engineering applications practically. As the most representative characteristic, the sensitivity of the prototypes is examined experimentally. If there are no extra constraints, the sensitivity should be as high as possible in general. Many factors will affect the sensitivity of the present sensor such as yoke dimensions, performance of permanent magnets, the number of turns of the solenoid coil, the gap between the shaft and the magnets, and so on. Among these factors the strength of the bias magnetic fields is expected to be the most influential. With a view to examining the sensitivity variation, the output voltages

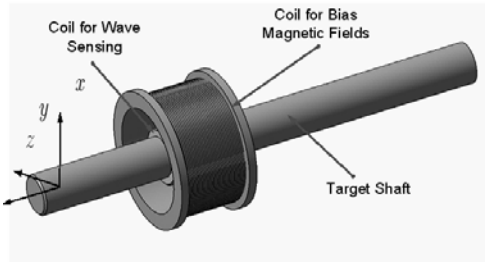

Fig. 10. Sensor configuration in order to examining the sensitivity of the proposed sensor.

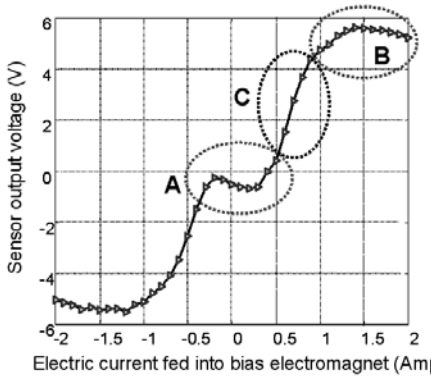

Fig. 11. Variation of the sensor output voltages according to the electric current fed into the bias electromagnet.

are measured according to the variation of the bias magnetic field strength. For all the experiments, the ball drop height remains fixed for consistency. Since permanent magnets are not appropriate for these experiments, electromagnets to vary the bias magnet field must be constructed. The solenoid-type electromagnet shown in Fig. 10 is constructed. Since an electromagnet will produce constant bias magnetic fields in the z direction at the cross section of the sensing coil, it will be representative of the symmetric bias magnetic fields. Although the experiments using a solenoid-type electromagnet are carried out only for the longitudinal mode, the same arguments will be valid for the flexural case since the basic principle is the same for the two sensing modes.

The output voltage variations are plotted in Fig. 11 according to the electric current fed into the electromagnet. Three design guides can be asserted from this result. First, the area A should be avoided because the sensitivity is very low and exceedingly nonlinear. Second, the area B is also not appropriate as a design candidate because of nonlinearity in spite of its high sensitivity. Lastly the area C is the most suitable for magnetic circuit designs in that the sensitivity of that

area is relatively high and fairly linear.

3.3 Linearity

All sensors should have linear relation between their inputs and outputs. It is worth noting that the linearity is different from the linearity of the sensitivity in 3.2. Especially, if the present sensor is used in the nondestructive evaluation, the linearity should be guaranteed for quantitative evaluations. The experiments shown in Fig. 12 are carried out in order to verify the linearity. Namely, the outputs are recorded as the height of the ball drops is controlled. If the ball drops with an angle α (see Fig. 12), the velocity immediately before the collision of the ball is given by the following expression:

$$V = \sqrt{2g(1-\cos\alpha)} \quad \text{(m/sec)} \tag{1}$$

where g is the gravitational acceleration. The impact of the ball with velocity V will produce longitudinal waves. Using the 1st order approximation, the stress level σ of the longitudinal waves is expressed as [16]:

$$\sigma = \frac{1}{2}\rho c V \quad (\text{N/m}^2) \tag{2}$$

Here, ρ is the density of a shaft and c is the velocity of dilation waves progressing along the shaft. The values of this case are 7850kg/m^3 and 5060m/sec, respectively since the shaft is made of steel. Substituting Eq. (1) into Eq. (2) the following equation for will be obtained.

$$\sigma = \frac{1}{\sqrt{2}}\rho c\sqrt{g(1-\cos\alpha)} \quad (\text{N/m}^2) \tag{3}$$

If the relation between the stress σ and the output voltage v_{out} is linear, socalled, $v_{out} = K\sigma$, then Eq. (3) can be rewritten as

$$v_{out} = K\frac{1}{\sqrt{2}}\rho c\sqrt{g(1-\cos\alpha)} \tag{4}$$

From Eq. (3) and Eq. (4) if the output voltage obtained from the experiments matches Eq. (3) except linear scaling K, we can conclude that the relation between the stress level and the output voltage is linear. In Fig. 13 the experimental data and theoretical ones are compared with each other. The stress level for $\alpha = 20^\circ$ corresponds to 30MPa and $\alpha = 90^\circ$ to 124MPa from Eq. (3). From these results, it can be concluded that the sensor exhibits linear responses for the stress range between 30 MPa and 124 MPa.

3.4 Rejection capability against undesirable waves

The essential point of the present paper is mode-selectivity. If we configure the sensor with the longitudinal sensing mode, then the flexural waves are not measured and vice versa. In order to confirm the selectivity and examine to what degree undesirable waves are rejected, the experiments depicted in Fig. 14 are carried out. First, the sensor is set to longitudinal sensing mode and perfectly flexural waves are generated by the ball drop as shown in Fig. 14. If the present sensor has good mode selectivity, no signals will be measured under this longitudinal sensing

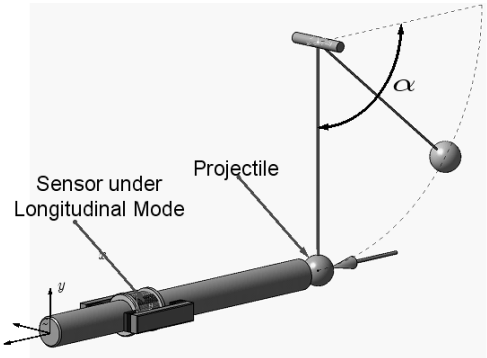

Fig. 12. Experimental configuration for examining the linearity of the proposed sensor.

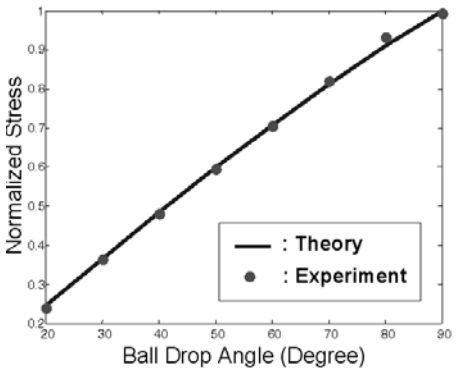

Fig. 13. Comparison between theory and experimental results to verify the linearity.

Table 2. Mode rejection ratios against the undesirable modes.

	Longitudinal Sensing Mode	Flexural Sensing Mode
Longitudinal Wave Signal	1	0.077
Flexural Waves Signal	0.018	1

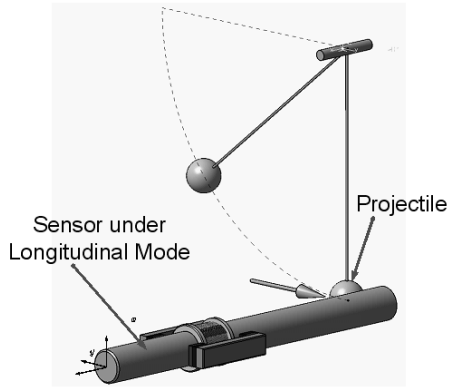

Fig. 14. Experimental configuration for examining the rejection capability against undesirable modes.

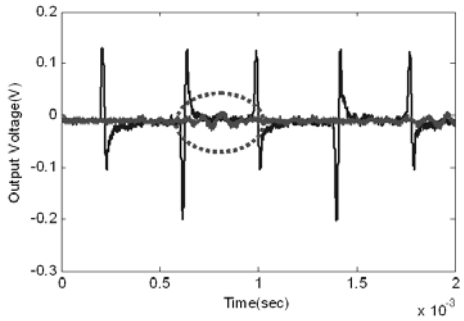

(a)

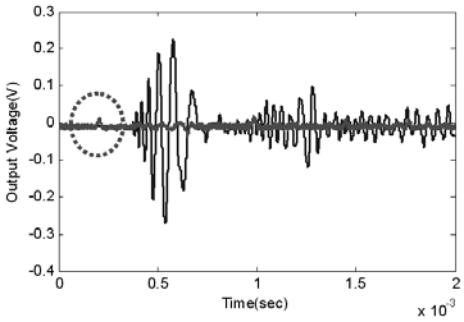

(b)

Fig. 15. Mode rejection results; (a) the longitudinal sensing mode can reject flexural waves and (b) flexural sensing mode can reject longitudinal waves.

mode. On the contrary, if the sensor is configured as the flexural sensing mode and the experimental setup of Fig. 12 is used , we will also get no signals from the sensor. In all the experiments, the angle of ball drops is fixed to 80° for consistency. The results are represented in Fig. 15. Fig. 15(a) is for the case of longitudinal sensing mode and flexural mode excitation. The dotted circle indicates the evidence of flexural waves but their magnitude is considerably attenuated as expected. The result of the longitudinal sensing mode is displayed as well for comparison. The case of flexural sensing mode and longitudinal mode excitation is also given in Fig. 15(b). Similarly, longitudinal waves are measured (see the dotted circles) but their amplitude is negligible. The maximum amplitudes of each wave modes are extracted and normalized with respect to the data from the appropriate setting. Here, the term of 'appropriate setting' means that the longitudinal sensing mode is used for longitudinal waves and the same for the flexural case. Table 2 represents the results. We can find that undesirable wave modes are rejected by the sensor in the ratio of at least 1/10 or at most 1/50.

4. Conclusions and future work

A sensor has been proposed for wave mode selection in a ferromagnetic shaft. The new sensor configuration is presented in which longitudinal waves and flexural ones can be selectively measured by the simple polarity reversions of bias magnets. In order to verify the proposed idea before prototyping, finite element analysis is carried out. From the finite element analysis the ideas are confirmed to be valid and some design guides are asserted. The sensor prototypes are made for experimental verification. The basic sensor characteristics such as sensitivity and linearity are examined experimentally. The ultimate goal of the present paper is verified by the rejection capability of the sensor against the undesirable wave. It is our future research goal to control the selectivity electrically by substituting the permanent magnets with electromagnets.

5. References

[1] J. O. Kim, and B. Bau, On line real-time desimeter-theory and optimization, *Journal of Acoustical Society of America*, 89 (1989) 432-439.

[2] W. J. Fleming, Computer-model simulation results

for three magnetostrictive torque sensor designs, *SAE Technical Papers*, (1991), 910857.

[3] H. Kwun and K. A. Bartel, Magnetostrictive sensor technology and its application," *Ultrasonics*, 36 (1998) 171-178.

[4] T. B. Thoe, D. K. Aspinwall and M. L. H. Wise, Review on ultrasonic machining, *International Journal of Machine Tools and Manufacture*, 38 (4) (1998) 239-255.

[5] W. Liu, L. Zhou, T. Xia, and H. Yu, Rare earth ultrasonic transducer technique research, *Ultrasonics*, 44 (Sup.1) (2006) e689-692.

[6] I. J. Garshelis and C. A. Jones, Miniaturized magnetoelastic torque transducer, *IEEE Transactions On Magnetics*, 35 (5) (1999) 3649-3651.

[7] D. K. Kleinke, and H. M. Uras, A noncontacting magnetostrictive strain sensor, *Review of Scientific Instruments*, 64 (8) (1993) 2361-2367.

[8] R. Murayama, Study of driving mechanism in electromagnetic acoustics transducer for Lamb wave using magnetostrictive effect and application in drawability evaluation of thin steel sheets, *Ultrasonics*, 37 (1999) 31-38

[9] H. Kwun, S. Y. Kim and J. F. Crane, Method and apparatus generating and detecting torsional wave inspection of pipes or tubes, *US Patent* No. 6,429,659 B1.

[10] Y. Y. Kim, S. H. Cho and H. C. Lee, Application of magnetomechanical sensors for modal testing, *Journal of Sound and Vibration*, 268 (2003) 799-808.

[11] S. W. Han, H. C. Lee and Y. Y. Kim, Noncontact damage detection of a rotating shaft using the magnetostrictive effect, *Journal of Nondestructive Evaluation*, 22(4) (2003) 141-151.

[12] J. S. Lee, S. H. Cho and Y. Y. Kim, Radiation pattern of Lamb waves generated by a circular magnetostrictive patch transducer, *Applied Physics Letters*, 90 (2007) 054101-1-3.

[13] K. F Graff, Wave motion in elastic solids, Dover Publications Inc., New York, USA, (1991).

[14] H. Kwun and C. M. Teller, Magnetostrictive generation and detection of longitudinal, torsional, and flexural waves in a rod, *Journal of Acoustical Society of America*, 96 (1994) 1202-1204.

[15] H. Lee and Y. Y. Kim, Wave selection using a magnetomechanical sensor in a solid cylinder, *Journal of Acoustical Society of America*, 112 (2002) 953-960.

[16] M. A. Meyers, Dynamic Behaviors of Materials, Wiley-Interscience, New York, USA. (1994) Chap. 2.